ResearchGate

See discussions, stats, and author profiles for this publication at: https://www.researchgate.net/publication/342674422

Numerical investigation of space fractional order diffusion equation by the Chebyshev collocation method of the fourth kind and compact finite difference scheme

Article *in* Discrete and Continuous Dynamical Systems - Series S · July 2020

DOI: 10.3934/dcdss.2020402

CITATIONS
3

READS
111

5 authors, including:

Yones Esmaeelzade Aghdam
Shahid Rajaee University
26 PUBLICATIONS **139** CITATIONS
SEE PROFILE

Hamid Safdari
Shahid Rajaee University
17 PUBLICATIONS **81** CITATIONS
SEE PROFILE

Hossein Jafari
University of Mazandaran
306 PUBLICATIONS **7,795** CITATIONS
SEE PROFILE

Some of the authors of this publication are also working on these related projects:

A Recursive Solution Approach to Linear Systems with Non-Zero Minors View project

2nd International Conference on “Orthogonal Polynomials, Special Functions and Computer Algebra: Applications in Engineering” from October 15th-16th, 2022 at Jaipur, Rajasthan, INDIA||https://anandice.ac.in/opsfca2022/ View project

All content following this page was uploaded by Yones Esmaeelzade Aghdam on 09 July 2020.

The user has requested enhancement of the downloaded file.

DISCRETE AND CONTINUOUS
DYNAMICAL SYSTEMS SERIES S

doi:10.3934/dcdss.2020402

NUMERICAL INVESTIGATION OF SPACE FRACTIONAL ORDER DIFFUSION EQUATION BY THE CHEBYSHEV COLLOCATION METHOD OF THE FOURTH KIND AND COMPACT FINITE DIFFERENCE SCHEME

Yones Esmaeelzade Aghdam, Hamid Safdari* and Yaqub Azari

Department of Mathematics, Shahid Rajaee Teacher Training University
Tehran, Iran

Hossein Jafari

Department of Mathematics, University of Mazandaran, Babolsar, Iran
Department of Mathematical Sciences, University of South Africa
UNISA 0003, South Africa

Dumitru Baleanu

Department of Mathematics, Cankaya University, Ankara, Turkey
Institute of Space Sciences, Magurele-Bucharest, Romania

Abstract. This paper develops a numerical scheme for finding the approximate solution of space fractional order of the diffusion equation (SFODE). Firstly, the compact finite difference (CFD) with convergence order $\mathcal{O}(\delta\tau^2)$ is used for discretizing time derivative. Afterwards, the spatial fractional derivative is approximated by the Chebyshev collocation method of the fourth kind. Furthermore, time-discrete stability and convergence analysis are presented. Finally, two examples are numerically investigated by the proposed method. The examples illustrate the performance and accuracy of our method compared to existing methods presented in the literature.

1. **Introduction.** One of the issues which have garnered researchers' attention these days is the fractional differential equations (FDEs) and have been numerically investigated by a huge number of authors [2, 3, 8, 9, 16, 21, 23, 25, 28, 29]. Fractional calculus is involved in many applications of science and engineering such as economics, physics, optimal control, and other applications, see [10, 11, 13, 19, 22, 26, 33, 34, 35]. A case in point is the diffusion and reaction-diffusion models in the physical environment.

These models in physics explain the action of the plural motion of micro-particles in a material eventuating arising from the random motion of each micro-particle. Moreover, it is suitable as a topic related to the Markov process in mathematics as well as in various fields, such as social science, life science, materials sciences, information science, etc. These subjects can be explained using the diffusion equations named Brown equations.

2020 *Mathematics Subject Classification.* 34K37, 91G80, 97N50.

Key words and phrases. Space fractional order diffusion equation, compact finite difference, Chebyshev collocation method of the fourth kind, convergence, stability.

* Corresponding author: Hamid Safdari.

Space fractional order of the diffusion equations (SFODEs) as fractional partial differential equations are numerically investigated by a large number of research papers, see for instance [15, 29, 30, 31].

In the last decades, spectral methods are increasingly used for approximating the solution of the ordinary differential equations (ODEs) and partial differential equations (PDEs), etc. The spectral methods have become popular because of finding accurate results with fewer degrees of freedom for solving the PDEs [4, 5, 20].

The Chebyshev polynomials (CPs) as the orthogonal polynomials, in spectral methods, are used for finding the approximation of functions on the interval $[-1, 1]$, see [1, 12, 14]. Because there is the powerful relation of these polynomials with Laurent and Fourier series, they have many applications in ODEs and PDEs. The CPs have four kinds, see [20], that we are dealing with the fourth one and call it CPF.

In recent years, the various methods have been implemented for solving SFODEs. Tadjeran et al. in [32] combined the classical Crank-Nicholson method and spatial extrapolation to get the approximate solution of the SFODE. In [27], authors utilized the shifted Legendre-tau for solving SFODE. The references [15], [30], as well as [31] applied new closed formulae for approximating SFODEs by shifted CPs of the first, second, and third kinds, respectively. They obtained a linear order for the time derivative.

We consider the following of SFODE with the initial and boundary conditions as follows

$$\frac{\partial u(x,t)}{\partial t} = q(x)\frac{\partial^\alpha u(x,t)}{\partial x^\alpha} + p(x,t), \quad 0 < x < 1, \quad 0 < t \leq T, \tag{1}$$

$$u(x,0) = g(x), \quad 0 < x < 1, \tag{2}$$

$$u(0,t) = \varphi_0(t), \quad u(1,t) = \varphi_1(t), \quad 0 < t \leq T, \tag{3}$$

where $p(x,t)$ and the parameter α $(1 < \alpha < 2)$ are the source term and fractional order, respictively. We should mentioned that with $\alpha = 2$, Eq. (1) will be the classical diffusion equation. Here $\frac{\partial^\alpha u(x,t)}{\partial x^\alpha}$ is the Caputo fractional derivative of order α. The left Caputo's derivative of fractional order $\alpha \in \mathbb{R}^+$ is defined as

$${}_0^C\mathcal{D}_x^\alpha u(x,t) = \begin{cases} \frac{1}{\Gamma(n-\alpha)} \int_0^x (x-y)^{n-\alpha-1} \frac{\partial^n u(y,t)}{\partial y^n} dy, & n-1 < \alpha \leq n, \ n \in \mathbb{N}, \\ \frac{\partial^n u(x,t)}{\partial x^n}, & \alpha = n. \end{cases}$$

For simplicity, we use $\mathcal{D}^\alpha$ instead of ${}_0^C\mathcal{D}_x^\alpha$. It is listed some properties of the Caputo fractional derivative $\mathcal{D}^\alpha$ as [6, 17, 24]:

1. $\mathcal{D}^\alpha x^\beta = \frac{\Gamma(1+\beta)}{\Gamma(1+\beta-\alpha)} x^{\beta-\alpha}, \quad 0 < \alpha < \beta + 1, \ \alpha > -1,$

2. $\mathcal{D}^\alpha(\gamma f(x,t) + \varsigma g(x,t)) = \gamma \mathcal{D}^\alpha f(x,t) + \varsigma \mathcal{D}^\alpha g(x,t),$

3. $\mathcal{D}^\alpha(C) = 0,$ C is a constant.

The motivation of this paper is based on applying compact finite difference (CFD) for time-discretizing of SFODEs and displaying the unconditional stability of the method as well as proving the convergence order of $\mathcal{O}(\delta\tau^2)$, while the existing methods give the order $\mathcal{O}(\delta\tau^2)$. We formulate the fractional derivative of the Chebyshev polynomials of the fourth-kind by the properties of the Caputo derivative. We next implement the CPF by collocation method for spatial-discretizing to obtain a

full-discretization relation. The presented stability, convergence analysis and solved numerical examples display the excellent performance of our method.

The structure of the paper is outlined as follows. Section 2 summarizes some properties of the CPF and presents a closed formula of the fractional derivative. In Section 3, we approximate the fractional derivative $\frac{\partial^\alpha u}{\partial x^\alpha}$ and explain the application of the Chebyshev collocation method for solving Eq. (1). Moreover, the CFD and shifted Chebyshev polynomials of the fourth kind (SCPF) are implemented to discrete in time and space direction, respectively. In Section 4, we discuss the convergence analysis and stability of the proposed method and display the stability of the method is unconditional and the convergence order of the time derivative is $\mathcal{O}(\delta\tau^2)$. Section 5 illustrates the accuracy and efficiency of the proposed method with two numerical experiments.

2. **Some properties of CPF.** In this section, we list some properties of the CPs of the fourth kind. We first define the Jacobi polynomials $\mathcal{P}_i^{(a,b)}(x)$ as

$$\mathcal{P}_i^{(a,b)} = \frac{\Gamma(a+i+1)}{i!\Gamma(a+b+i+1)} \sum_{m=0}^{i} \binom{i}{m} \frac{\Gamma(a+b+i+m+1)}{\Gamma(a+m+1)} \times (\frac{x-1}{2})^m.$$

These polynomials are orthogonal with respect to the Jacobi weight function $\omega^{(a,b)}(x) = (1-x)^a(1+x)^b$ on the interval $[-1,1]$. The CPFs $W_i(x)$ are defined based on the Jacobi polynomials $\mathcal{P}_i^{(a,b)}(x)$ as below

$$W_i(x) = \frac{2^{2i}}{\binom{2i}{i}} \mathcal{P}_i^{(\frac{1}{2},\frac{-1}{2})}(x).$$

Using analytical form of the the above equation, the CPFs $W_i(x)$ of degree i can be rewritten as follows:

$$\begin{aligned} W_i(x) &= \frac{(2^{2i-2})\Gamma(i+0.5)(i-1)!}{(2i-2)!} \\ &\quad \times \sum_{k=0}^{i-1} \sum_{\xi=0}^{k} \frac{(-1)^\xi \Gamma(i+k)}{2^k k! \times (i-k-1)\Gamma(k+1.5)} \times \binom{k}{\xi} \times x^{k-\xi} \\ &= \Psi_i \sum_{k=0}^{i-1} \sum_{\xi=0}^{k} \Upsilon_{i,k,\xi} \times x^{k-\xi}, \quad i = 1, 2, \ldots, N+1, \end{aligned}$$

where $x \in [-1,1]$ and

$$\Psi_i = \frac{(2^{2i-2})\Gamma(i+0.5)(i-1)!}{(2i-2)!},$$

$$\Upsilon_{i,k,\xi} = \frac{(-1)^\xi \Gamma(i+k)}{2^k k! \times (i-k-1)\Gamma(k+1.5)} \times \binom{k}{\xi}.$$

We use the SCPF $W_i^*(x) = W_i(2x-1)$ defined by

$$W_i^*(x) = \Psi_i \sum_{k=0}^{i-1} \sum_{\xi=0}^{k} \Upsilon_{i,k,\xi} \times 2^k \times x^{k-\xi}, \quad x \in [0,1], \quad i = 1, 2, \ldots.$$

In addition, the SCPF is orthogonal on $[0,1]$ with the inner product

$$\langle W_i^*(x), W_j^*(x) \rangle = \int_0^1 \sqrt{\frac{1-x}{x}}\, W_i^*(x)\, W_j^*(x) dx = \begin{cases} 0, & i \neq j, \\ \frac{\pi}{2}, & i = j. \end{cases}$$

If $g(x)$ be a square-integrable on the interval $[0,1]$, then it can be expanded in series of the SCPF as follows [30]

$$g(x)=\sum_{i=0}^{\infty} w_i\, W_i^*(x), \quad x\in[0,1], \tag{4}$$

where the coefficients $w_i,\ i=0,1,2,\ldots,$ are defined by

$$w_i=\frac{2}{\pi}\int_0^1 \sqrt{\frac{1-x}{x}}\, g(x)\, W_i^*(x)dx. \tag{5}$$

It should be mentioned that in practice only N-terms of Eq. (4) are considered and explained more in the next section.

Now, we formulate the fractional derivative of $W_i^*(x)$ by the properties of the Caputo derivative as

$$\mathcal{D}^{\alpha}(W_i^*(x))=\sum_{k=0}^{i-\lceil\alpha\rceil}\sum_{\xi=0}^{k} N_{i,k,\xi}^{\alpha,\lceil\alpha\rceil}\times x^{k-\xi-\alpha+\lceil\alpha\rceil}, \quad x\in[0,1], \quad i=0,1,2,\ldots, \tag{6}$$

where $\lceil\alpha\rceil$ is the ceiling of α and $N_{i,k,\xi}^{\alpha,\lceil\alpha\rceil}$ is defined by

$$N_{i,k,\xi}^{\alpha,\lceil\alpha\rceil}=\frac{(-1)^{\xi}\ 2^{2i}\ (i)!\ \Gamma(i+0.5)\ \Gamma(i+k+\lceil\alpha\rceil+1)\ \Gamma(k-\xi+\lceil\alpha\rceil+1)}{(2i)!\ (i-k-\lceil\alpha\rceil)!\ (k+\lceil\alpha\rceil)!\ \Gamma(k+\lceil\alpha\rceil+1.5)\ \Gamma(k-\xi-\alpha+\lceil\alpha\rceil+1)} \times\binom{k+\lceil\alpha\rceil}{\xi}.$$

Notice that we have

$$\mathcal{D}^{\alpha}(W_i^*(x))=0, \quad i=0,1,2,\ldots,\lceil\alpha\rceil-1, \quad \alpha>0. \tag{7}$$

Combininig Eqs. (4) and (6), one can obtain

$$\mathcal{D}^{\alpha}(g(x))=\sum_{i=\lceil\alpha\rceil}^{\infty}\sum_{k=0}^{i-\lceil\alpha\rceil}\sum_{\xi=0}^{k} w_i\times N_{i,k,\xi}^{\alpha,\lceil\alpha\rceil}\times x^{k-\xi-\alpha+\lceil\alpha\rceil}, \quad x\in[0,1]. \tag{8}$$

3. **Description of the numerical method for SFODE.** In this section, we apply a method for solving Eq. (1) based on the CFD and using the Chebyshev collocation method of the fourth kind. For given two positive integers M and N, we introduce time-mesh points as $\tau_{j-1}=(j-1)\delta\tau$ for $j=1,2,\ldots,M+1$, in which $\delta\tau=\frac{T}{M}$. Also, we consider the collocation points $\{x_{r-1}\}_{r=1}^{N+1-\lceil\alpha\rceil}$ using the roots of the SCPF $W_{N+1-\lceil\alpha\rceil}^*(x)$.

For time-descretizing, we fisrt write $u(x,t)\in\mathbb{C}^3(0,1)$, based on Taylor expansion, as

$$\frac{\partial u(x_r,t_j)}{\partial t}=\delta_\tau u(x_r,t_j)+\frac{\delta\tau}{2}\frac{\partial^2 u(x_r,t_j)}{\partial t^2}+\mathcal{O}(\delta\tau^2), \tag{9}$$

where $\delta_\tau u(x_r,t_j)=\frac{u_r^j-u_r^{j-1}}{\delta\tau}$. Now, substituting (9) into (1), we get

$$\delta_\tau u(x_r,t_j)+\frac{\delta\tau}{2}\frac{\partial^2 u(x_r,t_j)}{\partial t^2}+\mathcal{O}(\delta\tau^2)=q(x_r)\frac{\partial^\alpha u(x_r,t_j)}{\partial x^\alpha}+p(x_r,t_j). \tag{10}$$

Also, the second time derivative of Eq. (1) will be obtained as

$$\frac{\partial^2 u(x_r,t_j)}{\partial t^2}=q(x_r)\delta_\tau\frac{\partial^\alpha u(x_r,t_j)}{\partial x^\alpha}+\delta_\tau p(x_r,t_j). \tag{11}$$

Substituting Eq. (11) into Eq. (10), we have

$$\begin{aligned}\delta_\tau u(x_r,t_j) &= q(x_r)\frac{\partial^\alpha u(x_r,t_j)}{\partial x^\alpha} + p(x_r,t_j)\\ &\quad - \frac{\delta\tau}{2}\Big(q(x_r)\delta_\tau\frac{\partial^\alpha u(x_r,t_j)}{\partial x^\alpha} + \delta_\tau p(x_r,t_j)\Big) + \dots.\end{aligned} \tag{12}$$

After time-discretizing Eqs. (12), denoting $u(x_r,t_j) = U_r^j$, $p(x_r,t_j) = p_r^j$, and sorting, we obtain the following semi-discrete form

$$U_r^j - \frac{\delta\tau}{2}q(x_r)\frac{\partial^\alpha U_r^j}{\partial x^\alpha} = U_r^{j-1} + \frac{\delta\tau}{2}q(x_r)\frac{\partial^\alpha U_r^{j-1}}{\partial x^\alpha} + \frac{\delta\tau}{2}(p_r^j + p_r^{j-1}) + \mathcal{R}^j(x)(\delta\tau)^3, \tag{13}$$

where $\mathcal{R}^j(x)$ is the truncation term. For obtaining full-discrete form we require to approximate the Caputo derivative in $\frac{\partial^\alpha U_r^j}{\partial x^\alpha}$. The approximate solution $u(x,t)$ is constructed by using the following Chebyshev collocation technique

$$u_N(x,t) = \sum_{i=0}^{N} \mathfrak{u}_i(t)\, W_i^*(x). \tag{14}$$

Based on Eqs. (8), (13), (14), and using the roots of SCPF $\{x_r\}_{r=1}^{N-1}$, one can simply obtain

$$\begin{aligned}&\sum_{i=0}^{N}\mathfrak{u}_i^j\, W_i^*(x_r) - \frac{\delta\tau}{2}q(x_r)\sum_{i=2}^{N}\sum_{k=0}^{i-2}\sum_{\xi=0}^{k}\mathfrak{u}_i^j \times N_{i,k,\xi}^{\alpha,2}\times x_r^{k-\xi-\alpha+2}\\ &= \sum_{i=0}^{N}\mathfrak{u}_i^{j-1}\, W_i^*(x_r) + \frac{\delta\tau}{2}q(x_r)\sum_{i=2}^{N}\sum_{k=0}^{i-2}\sum_{\xi=0}^{k}\mathfrak{u}_i^{j-1} \times N_{i,k,\xi}^{\alpha,2}\times x_r^{k-\xi-\alpha+2}\\ &+ \frac{\delta\tau}{2}(p(x_r,t_j) + p(x_r,t_{j-1})).\end{aligned} \tag{15}$$

where $\mathfrak{u}_i^j$ denotes the coefficients in the point of t_j. Afterwards, by substituting the boundary conditions (3), we have

$$u(0,t) = \sum_{i=0}^{N}(-1)^i\mathfrak{u}_i(t) = \varphi_0(t), \quad u(1,t) = \sum_{i=0}^{N}(2i+1)\mathfrak{u}_i(t) = \varphi_1(t). \tag{16}$$

Eq. (15) along with Eq. (16), give $N+1$ of linear algebraic equations which can be solved for obtaining the unknown $\mathfrak{u}_i$, $i = 0,1,2,\dots,N$. It should be mentioned that for getting the initial solution $\mathfrak{u}_i^0$ of Eq. (15), we use the initial condition of the problem i.e., $u(x,0)$ combining Eq. (5).

4. **Convergence analysis and stability of the method.** In this section, we investigate the convergence and stability of the proposed numerical method. Let Ω denotes an open and bounded domain in $\mathbb{R}^2$ space. Also, $L_2(\Omega)$ represents a Hilbert space with the following inner product

$$\langle u(x), v(x)\rangle = \int_\Omega u(x)v(x)dx,$$

and the Euclidean norm $\|u(x)\| = \langle u(x), u(x)\rangle^{\frac{1}{2}}$. In this paper, we define Sobolev space as

$$H^s(\Omega) = \{u \in L_2(\Omega), \frac{d^s u}{dx^s} \in L_2(\Omega)\}.$$

In this section, we suppose that $q(x)$ is nonnegative in SFODE for $0 \leq x \leq 1$. for investigating the stability and convergence analysis, we first begin by some following lemmas required.

Lemma 4.1. *For any $u, \nu \in H^{\frac{\alpha}{2}}(\Omega)$, we have*

$$\langle {}_a\mathcal{D}_x^{\alpha} u, \nu\rangle = \langle {}_a\mathcal{D}_x^{\frac{\alpha}{2}} u, {}_x\mathcal{D}_b^{\frac{\alpha}{2}} \nu\rangle, \quad \langle {}_x\mathcal{D}_b^{\alpha} u, \nu\rangle = \langle {}_x\mathcal{D}_b^{\frac{\alpha}{2}} u, {}_a\mathcal{D}_x^{\frac{\alpha}{2}} \nu\rangle, \quad \text{for } 1 < \alpha < 2,$$
$$\langle {}_a\mathcal{D}_x^{\alpha} u, {}_x\mathcal{D}_b^{\alpha} u\rangle = \cos(\alpha\pi)\|{}_a\mathcal{D}_x^{\alpha} u\|^2 = \cos(\alpha\pi)\|{}_x\mathcal{D}_b^{\alpha} u\|^2, \quad \text{for } \alpha > 0.$$

Proof. See [7]. □

Lemma 4.2. *For the functions $g(x)$ and ${}_a\mathcal{D}_x^{\alpha} g(x) \in H^{\alpha}(\Omega)$, there exists a sufficiently small enough $\delta\tau$ such that it holds*

$$\|g(x) + \frac{\delta\tau}{2} q(x_r)\ {}_a\mathcal{D}_x^{\alpha} g(x)\| \leq \|g(x)\|, \quad \text{for } 1 < \alpha < 2.$$

Proof. According to Lemma 4.1, one obtains

$$\begin{aligned}
\|g(x) + \frac{\delta\tau}{2} q(x_r)\ {}_a\mathcal{D}_x^{\alpha} g(x)\|^2 &= \langle g(x) + \frac{\delta\tau}{2} q(x_r)\ {}_a\mathcal{D}_x^{\alpha} g(x),\ g(x) + \frac{\delta\tau}{2} q(x_r) {}_a\mathcal{D}_x^{\alpha} g(x)\rangle \\
&= \|g(x)\|^2 + \delta\tau q(x_r)\langle {}_a\mathcal{D}_x^{\frac{\alpha}{2}} g(x),\ {}_x\mathcal{D}_b^{\frac{\alpha}{2}} g(x)\rangle + \frac{(\delta\tau)^2}{4} q(x_r)^2 \|{}_a\mathcal{D}_x^{\alpha} g(x)\|^2 \\
&= \|g(x)\|^2 + \delta\tau q(x_r) cos(\frac{\alpha}{2}\pi)\|{}_a\mathcal{D}_x^{\frac{\alpha}{2}} g(x)\|^2 + \frac{(\delta\tau)^2}{4} q(x_r)^2 \|{}_a\mathcal{D}_x^{\alpha} g(x)\|^2,
\end{aligned}$$

So, there is a small enough $\delta\tau$ such that the following inequality holds

$$\delta\tau q(x_r) cos(\frac{\alpha}{2}\pi)\|{}_a\mathcal{D}_x^{\frac{\alpha}{2}} g(x)\|^2 + \frac{(\delta\tau)^2}{4} q(x_r)^2 \|{}_a\mathcal{D}_x^{\alpha} g(x)\|^2 < 0,$$

that completes the desired proof. □

Lemma 4.3. *Let $U^j \in H^1(\Omega),\ j = 1, 2, \ldots, M$ and U^0 be the solution of Eq. (13) and the initial condition, respectively. Then the following inequality holds*

$$\|U^j\| \leq \|U^0\| + \max_{0 \leq r \leq N} \frac{\delta\tau}{2}(\|p_r^j\| + \|p_r^{j-1}\|), \tag{17}$$

where $U^j = u(x, t_j)$.

Proof. For the proof, the mathematical induction on j is implemented in what follows. For $j = 1$ in Eq. (13), we have

$$U^1 - \frac{\delta\tau}{2} q(x_r)\ {}_a\mathcal{D}_x^{\alpha} U^1 = U^0 + \frac{\delta\tau}{2} q(x_r)\ {}_a\mathcal{D}_x^{\alpha} U^0 + \frac{\delta\tau}{2}(p^1 + p^0), \tag{18}$$

multiplying Eq. (18) by U^1 and integrating on Ω, we conclude

$$\begin{aligned}
\|U^1\|^2 - \frac{\delta\tau}{2} q(x_r)\langle {}_a\mathcal{D}_x^{\alpha} U^1, U^1\rangle = \langle U^0, U^1\rangle &+ \frac{\delta\tau}{2} q(x_r)\langle {}_a\mathcal{D}_x^{\alpha} U^0, U^1\rangle \\
&+ \frac{\delta\tau}{2}(\langle p^1, U^1\rangle + \langle p^0, U^1\rangle).
\end{aligned} \tag{19}$$

We know that $\cos(\frac{\alpha}{2}\pi) < 0$ for $1 < \alpha < 2$. So based on Lemmas 4.1, we have

$$\langle {}_a\mathcal{D}_x^{\alpha} U^1, U^1\rangle = \langle {}_a\mathcal{D}_x^{\frac{\alpha}{2}} U^1, {}_x\mathcal{D}_b^{\frac{\alpha}{2}} U^1\rangle = \cos(\frac{\alpha}{2}\pi)\|{}_a\mathcal{D}_x^{\frac{\alpha}{2}} U^1\|^2 < 0.$$

Therefore for the left-hand side of Eq. (19), one can obtain

$$\|U^1\|^2 \leq \|U^1\|^2 - \frac{\delta\tau}{2} q(x_r)\langle {}_a\mathcal{D}_x^{\alpha} U^1, U^1\rangle. \tag{20}$$

Furthermore according to Lemma 4.2 and using Cauchy-Schwarz inequality for the right-hand side of Eq. (19), we can get

$$\begin{aligned}&\|\langle U^0, U^1\rangle + \frac{\delta\tau}{2}q(x_r)\langle\ {}_a\mathcal{D}_x^\alpha U^0, U^1\rangle\| \\ &\leq \|U^0 + \frac{\delta\tau}{2}q(x_r){}_a\mathcal{D}_x^\alpha U^0\|\|U^1\| \leq \|U^0\|\|U^1\|.\end{aligned} \tag{21}$$

So by utilizing Eqs. (19), (20), and (21), we can conclude

$$\|U^1\| \leq \|U^0\| + \max_{0\leq r\leq N}\frac{\delta\tau}{2}(\|p_r^j\| + \|p_r^{j-1}\|).$$

Suppose that Eq. (17) is true for all $k = 1, 2, \ldots, j-1$ as

$$\|U^k\| \leq \|U^0\| + \max_{0\leq r\leq N}\frac{\delta\tau}{2}(\|p_r^k\| + \|p_r^{k-1}\|). \tag{22}$$

Now by multiplying Eq. (13) by U^j and integrating on Ω, one can get

$$\begin{aligned}\|U^j\|^2 - \frac{\delta\tau}{2}q(x_r)\langle{}_a\mathcal{D}_x^\alpha U^j, U^j\rangle &= \langle U^{j-1}, U^j\rangle + \frac{\delta\tau}{2}q(x_r)\langle{}_a\mathcal{D}_x^\alpha U^{j-1}, U^j\rangle \\ &+ \frac{\delta\tau}{2}(\langle p^j, U^j\rangle + \langle p^{j-1}, U^j\rangle).\end{aligned}$$

Similar to the above procedure, we arrive at Using the Cauchy–Schwarz inequality, Lemma 4.2, Eq. (22) and following again above process, it leads that

$$\|U^j\| \leq \|U^{j-1}\| + \max_{0\leq r\leq N}\frac{\delta\tau}{2}(\|p_r^j\| + \|p_r^{j-1}\|).$$

which clearly leads to the proof of the Lemma. □

Theorem 4.4. *The numerical method introduced by Eq. (13) is unconditionally stable.*

Proof. Suppose that $U_r^j,\ j = 1, 2, \ldots, M$ be the approximate solution of the method obtained by Eq. (13) with the initial condition $U_r^0 = u(x_r, 0)$, then the error $\varepsilon^j = u(x_r, t_j) - U_r^j$ satisfies

$$\varepsilon^j - \frac{\delta\tau}{2}q(x_r)\frac{\partial^\alpha\varepsilon^j}{\partial x^\alpha} - \frac{\delta\tau}{2}q(x_r)\frac{\partial^\alpha\varepsilon^{j-1}}{\partial x^\alpha} = \varepsilon^{j-1}. \tag{23}$$

According to Lemma 4.3, we have

$$\|\varepsilon^j\| \leq \|\varepsilon^0\|, \quad j = 1, 2, \ldots, M,$$

which completes the proof of the unconditional stability of the scheme. □

Theorem 4.5. *If $\varepsilon^j = u(x, t_j) - U^j,\ j = 1, 2, \ldots, M$ be the errors for Eq. (13). Then we have*

$$\|\varepsilon^j\| \leq C^{'}(\delta\tau)^2,$$

where $C^{'}$ is a positive constant.

Proof. It is used the mathematical induction on j for the proof of the theorem. We can write the following error equation by using Eq. (13) as

$$\varepsilon^j - \frac{\delta\tau}{2}q(x_r)\mathcal{D}^\alpha\varepsilon^j = \varepsilon^{j-1} + \frac{\delta\tau}{2}q(x_r)\mathcal{D}^\alpha\varepsilon^{j-1} + \mathcal{R}^j(x)(\delta\tau)^3.$$

With multiplying above equation by ε^j and integrating, we get the following relation

$$\langle\varepsilon^j, \varepsilon^j\rangle - \frac{\delta\tau}{2}q(x_r)\langle\mathcal{D}^\alpha\varepsilon^j, \varepsilon^j\rangle = \langle\varepsilon^{j-1}, \varepsilon^j\rangle + \frac{\delta\tau}{2}q(x_r)\langle\mathcal{D}^\alpha\varepsilon^{j-1}, \varepsilon^j\rangle + (\delta\tau)^3\langle\mathcal{R}^j(x), \varepsilon^j\rangle.$$

Using the Cauchy-Schwarz inequality, Lemmas 4.1 and 4.2, we can write the following inequality

$$\|\varepsilon^j\|^2 \leq \|\varepsilon^{j-1}\|\|\varepsilon^j\| + (\delta\tau)^3\|\mathcal{R}^j(x)\|\|\varepsilon^j\|.$$

So, one can get

$$\|\varepsilon^j\| - \|\varepsilon^{j-1}\| \leq (\delta\tau)^3\|\mathcal{R}^j(x)\|, \implies \|\varepsilon^j\| - \|\varepsilon^{j-1}\| \leq C(\delta\tau)^3. \tag{24}$$

Summing relation (24) for j from 1 to M arrives at

$$\sum_{j=1}^{M}\left(\|\varepsilon^j\| - \|\varepsilon^{j-1}\|\right) \leq \sum_{j=1}^{M} C(\delta\tau)^3.$$

Thus, we can obtain

$$\|\varepsilon^M\| - \|\varepsilon^0\| \leq CM(\delta\tau)^3,$$

since $\|\varepsilon^0\| = 0$ and $\delta\tau = \frac{T}{M}$, we have

$$\|\varepsilon^M\| \leq C^{'}\delta\tau^2,$$

where $C^{'} = CT$ is a positive constant that depends on x. It concludes the proof of theorem 4.5. □

5. **Numerical results.** What we present in this section is to illustrate the efficiency of the method by some experiments. We give two examples of SFODE and indicate the accuracy of our scheme comparing to other schemes found in the literature. Moreover, the accuracy and stability of the proposed approach for various values of N and M is checked. In this paper, for comparing the accuracy of the methods the error norms L_∞ and L_2. Furthermore, we give the numerically computational orders and denote by $C_{\delta\tau}$ with the following formula

$$C_{\delta\tau} = \frac{\log(\frac{E_1}{E_2})}{\log(\frac{\delta\tau_1}{\delta\tau_2})},$$

where E_1 and E_2 are errors correspond to grids with mesh size $\delta\tau_1$ and $\delta\tau_2$, respectively.

Example 5.1. For the first example, we consider the following SFODE

$$\begin{aligned}&\frac{\partial u(x,t)}{\partial t} = \Gamma(1.2)x^{1.8}\frac{\partial^{1.8}u(x,t)}{\partial x^{1.8}} + 3x^2(2x-1)e^{-t}, \quad 0<x<1, \quad t>0,\\ &u(x,0) = x^2(1-x), \quad u(0,t) = u(1,t) = 0, \quad t>0,\end{aligned}$$

which has the exact solution $u(x,t) = x^2(1-x)e^{-t}$.

We report the results in Tables 1-5 at given various parameter. Tables 1 and 2 depict the comparison of the results obtained by our method with those achieved applying shifted CPs of the first kind in [15], shifted Legendre polynomials in [27] and shifted CPs of the second kind in [30] at $T = 1$ and $T = 2$, respectively. The results indicate our method gives much better results than other methods. In addition, Table 3 reports the absolute error calculated with $N = 3, 5, 7$ at $T = 10$ which displays the absolute error decreases when N increases. Tables 4 and 5 show the results obtained by the error norms L_∞, L_2, and the convergence order of the time derivative ($C_{\delta\tau}$) at $T = 1$ and $T = 10$, respectively. In these tables, the time convergence order denoted by TCO. The results confirm the convergence order of the time derivative in Theorem 4.5.

TABLE 1. The absolute error of Example 5.1 at $T = 1$.

x	with $N = 7$ in [15]	with $N = 7$ in [27]	with $N = 3$ in [30]	our method with $N = 3$
0	2.81×10^{-5}	0	0	4.77×10^{-17}
0.1	4.26×10^{-5}	4.66×10^{-5}	5.46×10^{-6}	3.17×10^{-9}
0.2	5.39×10^{-5}	7.74×10^{-5}	8.51×10^{-6}	5.85×10^{-9}
0.3	6.12×10^{-5}	5.00×10^{-5}	9.60×10^{-6}	7.97×10^{-9}
0.4	6.48×10^{-5}	2.30×10^{-5}	9.18×10^{-6}	9.44×10^{-9}
0.5	6.45×10^{-5}	2.74×10^{-5}	7.69×10^{-6}	1.02×10^{-8}
0.6	5.98×10^{-5}	4.38×10^{-5}	5.60×10^{-6}	1.01×10^{-8}
0.7	5.23×10^{-5}	3.87×10^{-5}	3.33×10^{-6}	9.12×10^{-9}
0.8	4.48×10^{-5}	1.01×10^{-5}	1.34×10^{-6}	7.17×10^{-9}
0.9	3.91×10^{-5}	3.35×10^{-5}	8.39×10^{-8}	4.16×10^{-9}
1.0	2.81×10^{-5}	0	0	7.55×10^{-17}

TABLE 2. The absolute error of Example 5.1 at $T = 2$.

x	with $N = 5$ in [15]	with $N = 5$ in [27]	with $N = 3$ in [30]	our method with $N = 3$
0	2.74×10^{-5}	0	0	1.86×10^{-17}
0.1	4.20×10^{-5}	4.47×10^{-6}	3.33×10^{-6}	1.28×10^{-8}
0.2	3.76×10^{-5}	2.78×10^{-7}	5.65×10^{-6}	2.05×10^{-8}
0.3	8.44×10^{-5}	5.81×10^{-6}	7.05×10^{-6}	2.40×10^{-8}
0.4	3.27×10^{-5}	1.02×10^{-5}	7.64×10^{-6}	2.40×10^{-8}
0.5	3.61×10^{-5}	1.17×10^{-5}	7.52×10^{-6}	2.15×10^{-8}
0.6	1.94×10^{-5}	1.08×10^{-5}	6.80×10^{-6}	1.72×10^{-8}
0.7	2.95×10^{-5}	8.54×10^{-6}	5.59×10^{-6}	1.21×10^{-8}
0.8	4.92×10^{-5}	6.06×10^{-6}	3.98×10^{-6}	6.93×10^{-9}
0.9	2.83×10^{-5}	3.67×10^{-6}	2.08×10^{-6}	2.62×10^{-9}
1.0	7.73×10^{-5}	0	0	8.24×10^{-18}

TABLE 3. The absolute error of Example 5.1 at $T = 10$.

x	$N = 3$	$N = 5$	$N = 7$
0	5.82×10^{-21}	5.93×10^{-22}	4.43×10^{-21}
0.2	1.01×10^{-9}	4.74×10^{-9}	2.28×10^{-9}
0.4	8.21×10^{-9}	8.11×10^{-9}	4.21×10^{-9}
0.6	1.28×10^{-9}	1.17×10^{-9}	1.15×10^{-9}
0.8	3.76×10^{-9}	7.93×10^{-10}	2.71×10^{-10}
1.0	4.34×10^{-21}	3.78×10^{-21}	1.14×10^{-22}

Figure 1 displays graphs of the absolute error and approximate solution using the CFD method with the Chebyshev collocation approach of the fourth kind with various parameters $M = 400$ and $N = 5$ at $T = 1$. In addition, Figure 2 depicts the error norm L_2 and L_∞ for Example 5.1 at $T = 1$, $N = 5$ and $M = 200, 400, 600, \ldots, 3000$. The error histories have been shown in Figure 3 at $T = 1$ for different values $N = 5$

TABLE 4. The convergence order, the errors L_2 and L_∞ for Example 5.1 with $T = 1$ and $N = 3$.

$\delta\tau$	L_∞	$C_{\delta\tau}$	L_2	$C_{\delta\tau}$
$\frac{1}{100}$	1.62773×10^{-7}		3.76647×10^{-7}	
$\frac{1}{200}$	4.06928×10^{-8}	2.00002	9.41607×10^{-8}	2.00002
$\frac{1}{400}$	1.01732×10^{-8}	2.00000	2.35401×10^{-8}	2.00000
$\frac{1}{800}$	2.54329×10^{-9}	2.00000	5.88503×10^{-9}	2.00000
$\frac{1}{1600}$	6.35828×10^{-10}	1.99999	1.47127×10^{-9}	1.99999
TCO		2		2

TABLE 5. The convergence order, the errors L_2 and L_∞ for Example 5.1 with $T = 10$ and $N = 3$.

$\delta\tau$	L_∞	$C_{\delta\tau}$	L_2	$C_{\delta\tau}$
$\frac{1}{100}$	1.63402×10^{-7}		3.10926×10^{-7}	
$\frac{1}{200}$	4.08673×10^{-8}	1.99941	7.77632×10^{-8}	1.99941
$\frac{1}{400}$	1.02179×10^{-8}	1.99985	1.94428×10^{-8}	1.99985
$\frac{1}{800}$	2.55453×10^{-9}	1.99996	4.86082×10^{-9}	1.99996
$\frac{1}{1600}$	6.38636×10^{-10}	1.99999	1.21521×10^{-9}	1.99999
TCO		2		2

and $M = 100, 200, 400, 800, 1600$. Also, Figure 4 compares the absolute error at $T = 1$, $M = 400$ and $N = 3, 5, 7, 9$.

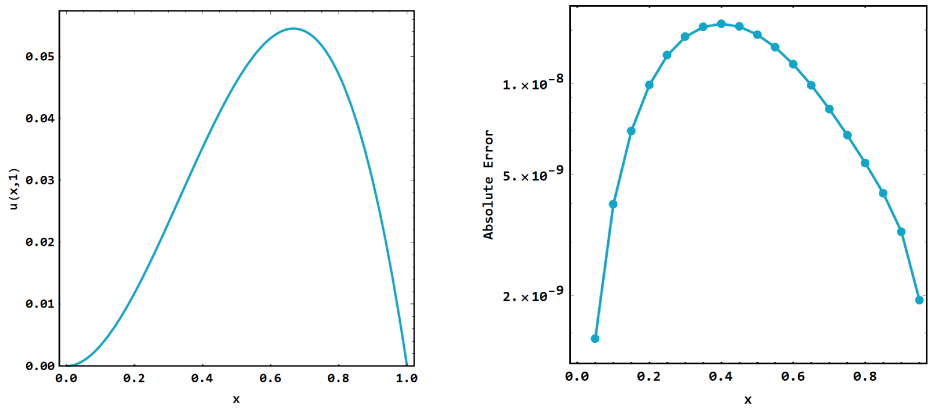

FIGURE 1. Plots of the approximate solution (left side) and absolute error (right side) of Example 5.1 at $T = 1$, $M = 400$ and $N = 5$.

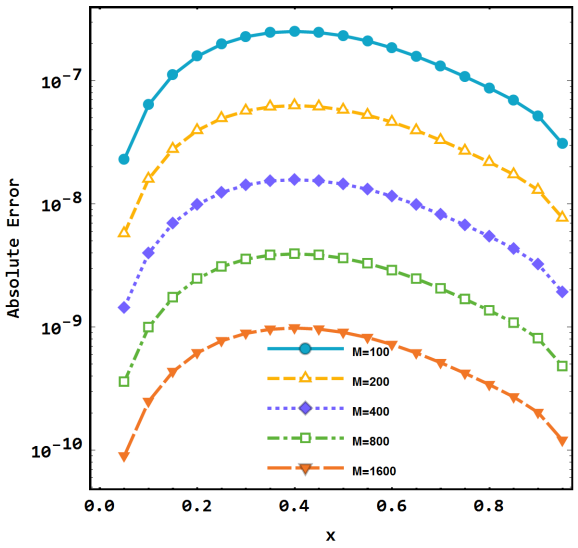

FIGURE 3. Error histories of Example 5.1 at $T = 1$, $N = 5$ and $M = 100, 200, 400, 800, 1600$.

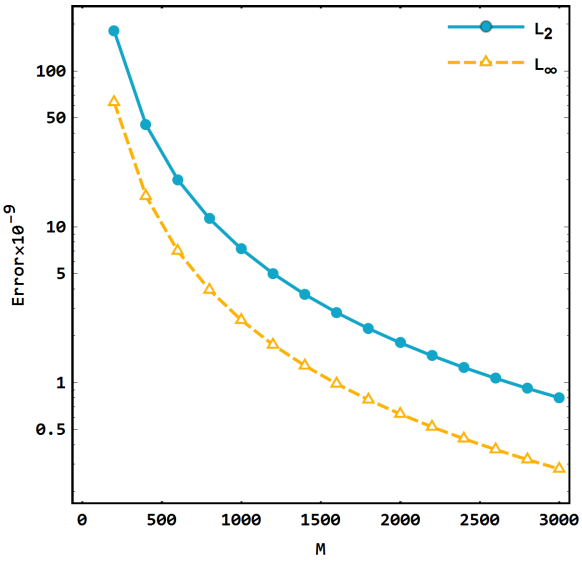

FIGURE 2. The maximum absolute error and error norm L_2 of Example 5.1 at $T = 1$, $N = 5$ and $M = 200, 400, 600, \ldots, 3000$.

Example 5.2. We consider the following SFODE as

$$\begin{aligned} &\frac{\partial u(x,t)}{\partial t} = \frac{\Gamma(2.2)}{6} x^{2.8} \frac{\partial^{1.8} u(x,t)}{\partial x^{1.8}} - x^3 e^{-t}(x+1), \quad 0 < x < 1, \quad t > 0, \\ &u(x,0) = x^3, \ u(0,t) = 0, \ u(1,t) = \exp(-t), \ t > 0, \end{aligned} \tag{25}$$

which exact solution given by $u(x,t) = x^3 e^{-t}$.

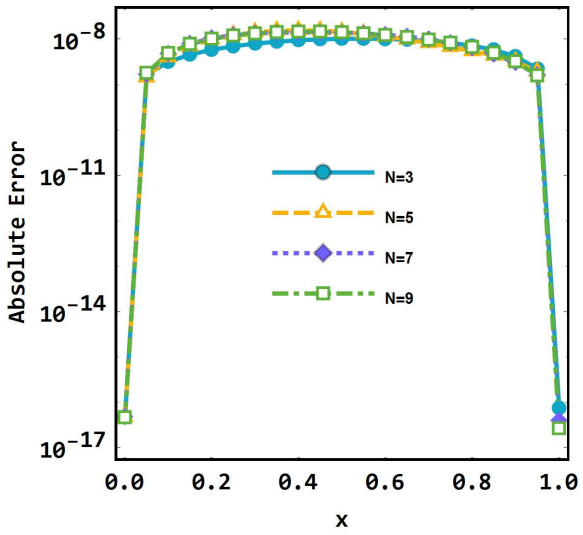

FIGURE 4. Error histories of Example 5.1 at $T = 1$, $M = 400$ and $N = 3, 5, 7, 9$.

TABLE 6. The convergence order, the errors L_2 and L_∞ for Example 5.2 with $N = 7$ at $T = 1$.

$\delta\tau$	L_∞	$C_{\delta\tau}$	L_2	$C_{\delta\tau}$
$\frac{1}{100}$	1.71816×10^{-6}		3.73349×10^{-6}	
$\frac{1}{200}$	4.29538×10^{-7}	2.00000	9.33372×10^{-7}	2.00000
$\frac{1}{400}$	1.07384×10^{-7}	2.00000	2.33343×10^{-7}	2.00000
$\frac{1}{800}$	2.68460×10^{-8}	2.00000	5.83360×10^{-8}	2.00000
$\frac{1}{1600}$	6.71143×10^{-9}	2.00002	1.45842×10^{-8}	1.99998
TCO		2		2

Table 6 represents the results of Example 5.2 with $N = 7$, $T = 1$, and various parameter $\delta\tau$. Furthermore based on the obtained results, the convergence order of the time derivative in Theorem 4.5, that is, $\mathcal{O}(\delta\tau^2)$ is supported. Table 7 compares the maximum error of our method with those found in [32] for Example 5.2 at $T = 1$ with $N = 7$. It is clearly observed that our approach presents more accurate results than those calculated by Crank–Nicolson scheme in [32]. Figure 5 indicates graphs of the numerical results at $T = 1$ for values $N = 5, 7$ and $M = 100, 200, 400, 800, 1600$.

6. **Conclusion.** This paper presented the Chebyshev polynomials of the fourth kind to approximate the SFODE. Firstly, the CFD is utilized to discrete temporal direction with order $\mathcal{O}(\delta\tau^2)$. Then, the space fractional derivative is approximated using Chebyshev collocation of the fourth kind. The unconditional stability of the proposed scheme has been analyzed in an appropriate Sobolev space. Finally, the numerical results are illustrated to confirm the efficiency and accuracy of the proposed method. As can be seen in the numerical results tables and figures, our

TABLE 7. The comparison of maximum error of our proposed method and [32] for Example 5.2, at $T = 1$.

Max error-CN [32]	Max error-ext CN [32]	the present method with N=3
6.84895×10^{-4}	2.82750×10^{-5}	9.95930×10^{-8}

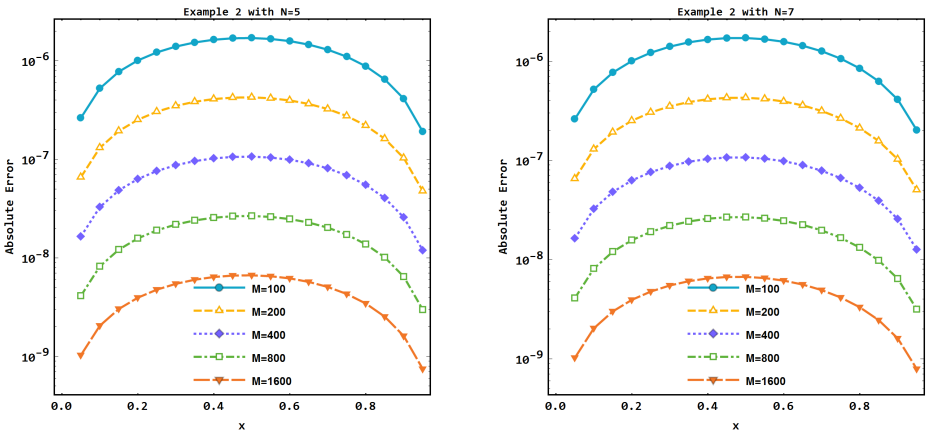

FIGURE 5. Error histories of Example 5.2 at $T = 1$, with $M = 100, 200, 400, 800, 1600$, $N = 5$ (left side) and $N = 7$ (right side).

method performs much better than other methods and yields far better results. So, the approach applied in this paper can be extended to other fractional models.

Acknowledgments. The authors would like to thank the two anonymous reviewers for their helpful comments.

REFERENCES

[1] M. Abdelhakem, H. Moussa, D. Baleanu and M. El-Kady, Shifted Chebyshev schemes for solving fractional optimal control problems, *Journal of Vibration and Control*, **25** (2019), 2143–2150.

[2] M. Badr, A. Yazdani and H. Jafari, Stability of a finite volume element method for the time–fractional advection–diffusion equation, *Numerical Methods for Partial Differential Equations*, **34** (2018), 1459–1471.

[3] V. O. Bohaienko, A fast finite-difference algorithm for solving space-fractional filtration equation with a generalised Caputo derivative, *Comput. Appl. Math.*, **38** (2019), 105, 21 pp.

[4] J. P. Boyd, *Chebyshev and Fourier Spectral Methods*, Second edition. Dover Publications, Inc., Mineola, NY, 2001.

[5] C. Canuto, M. Y. Hussaini, A. Quarteroni and T. A. Zang, *Spectral Methods*, Evolution to complex geometries and applications to fluid dynamics. Scientific Computation. Springer, Berlin, 2007.

[6] M. Caputo, Linear models of dissipation whose Q is almost frequency independent–ii, *Geophysical Journal International*, **13** (1967), 529–539.

[7] V. J. Ervin, N. Heuer and J. P. Roop, Numerical approximation of a time dependent, nonlinear, space-fractional diffusion equation, *SIAM J. Numer. Anal.*, **45** (2007), 572–591.

[8] R. M. Ganji and H. Jafari, Numerical solution of variable order integro-differential equations, *Advanced Mathematical Models & Applications*, **4** (2019), 64–69.
[9] M. M. Ghalib, A. A. Zafar, Z. Hammouch, M. B. Riaz and K. Shabbir, Analytical results on the unsteady rotational flow of fractional-order non-Newtonian fluids with shear stress on the boundary, *Discrete & Continuous Dynamical Systems - S*, **13** (2020), 683–693.
[10] A. Golbabai, O. Nikan and T. Nikazad, Numerical analysis of time fractional Black–Scholes european option pricing model arising in financial market, *Comput. Appl. Math.*, **38** (2019), Paper No. 173, 24 pp.
[11] A. Goswami, J. Singh, D. Kumar et al, An efficient analytical approach for fractional equal width equations describing hydro-magnetic waves in cold plasma, *Phys. A*, **524** (2019), 563–575.
[12] H. Hassani, J. A. Tenreiro Machado and E. Naraghirad, Generalized shifted Chebyshev polynomials for fractional optimal control problems, *Commun. Nonlinear Sci. Numer. Simul.*, **75** (2019), 50–61.
[13] B. I. Henry and S. L. Wearne, Existence of turing instabilities in a two-species fractional reaction-diffusion system, *SIAM J. Appl. Math.*, **62** (2001/02), 870–887.
[14] M. H. Heydari, A. Atangana and Z. Avazzadeh, Chebyshev polynomials for the numerical solution of fractal–fractional model of nonlinear Ginzburg–Landau equation, *Engineering with Computers*, (2019), 1–12.
[15] M. M. Khader, On the numerical solutions for the fractional diffusion equation, *Commun. Nonlinear Sci. Numer. Simul.*, **16** (2011), 2535–2542.
[16] M. A. Khan, Z. Hammouch and D. Baleanu, Modeling the dynamics of hepatitis e via the Caputo–Fabrizio derivative, *Math. Model. Nat. Phenom.*, **14** (2019), Paper No. 311, 19 pp.
[17] S. G. Samko, A. A. Kilbas and O. I. Marichev, *Fractional Integral and Derivatives, Theory and Applications*, Gordon and Breach Science Publishers, Yverdon, 1993.
[18] A. A. Kilbas, H. M. Srivastava and J. J. Trujillo, *Theory and Applications of Fractional Differential Equations*, North-Holland Mathematics Studies, 204. Elsevier Science B.V., Amsterdam, 2006.
[19] D. Kumar, J. Singh and D. Baleanu, On the analysis of vibration equation involving a fractional derivative with Mittag-Leffler law, *Math. Methods Appl. Sci.*, **43** (2020), 443–457.
[20] J. C. Mason and D. C. Handscomb, *Chebyshev Polynomials*, Chapman and Hall/CRC, Boca Raton, FL, 2003.
[21] O. Nikan, A. Golbabai, J. A. Tenreiro Machado and T. Nikazad, Numerical solution of the fractional Rayleigh–Stokes model arising in a heated generalized second-grade fluid, *Engineering with Computers*, (2020), 1–14.
[22] O. Nikan, J. A. Tenreiro Machado, A. Golbabai and T. Nikazad, Numerical approach for modeling fractal mobile/immobile transport model in porous and fractured media, *International Communications in Heat and Mass Transfer*, **111** (2020), 104443.
[23] K. M. Owolabi and A. Atangana, High-order solvers for space-fractional differential equations with Riesz derivative, *Discrete & Continuous Dynamical Systems-S*, **12** (2019), 567–590.
[24] I. Podlubny, *Fractional Differential Equations. An Introduction to Fractional Derivatives, Fractional Differential Equations, to Methods of their Solution and some of their Applications*, Mathematics in Science and Engineering, 198. Academic Press, Inc., San Diego, CA, 1999.
[25] L. Ren and L. Liu, A high-order compact difference method for time fractional Fokker–Planck equations with variable coefficients, *Comput. Appl. Math.*, **38** (2019), Paper No. 101, 16 pp.
[26] E. Reyes-Melo, J. Martinez-Vega, C. Guerrero-Salazar and U. Ortiz-Mendez, Application of fractional calculus to the modeling of dielectric relaxation phenomena in polymeric materials, *Journal of Applied Polymer Science*, **98** (2005), 923–935.
[27] A. Saadatmandi and M. Dehghan, A tau approach for solution of the space fractional diffusion equation, *Comput. Math. Appl.*, **62** (2011), 1135–1142.
[28] J. Singh, D. Kumar and D. Baleanu, New aspects of fractional Biswas–Milovic model with Mittag-Leffler law, *Math. Model. Nat. Phenom.*, **14** (2019), Paper No. 303, 23 pp.
[29] E. Sousa, Numerical approximations for fractional diffusion equations via splines, *Comput. Math. Appl.*, **62** (2011), 938–944.
[30] N. H. Sweilam, A. M. Nagy and A. A. El-Sayed, Second kind shifted Chebyshev polynomials for solving space fractional order diffusion equation, *Chaos Solitons Fractals*, **73** (2015), 141–147.

[31] N. Sweilam, A. Nagy and A. A. El-Sayed, On the numerical solution of space fractional order diffusion equation via shifted Chebyshev polynomials of the third kind, *Journal of King Saud University-Science*, **28** (2016), 41–47.
[32] C. Tadjeran, M. M. Meerschaert and H.-P. Scheffler, A second-order accurate numerical approximation for the fractional diffusion equation, *J. Comput. Phys.*, **213** (2006), 205–213.
[33] S. Ullah, M. Altaf Khan and M. Farooq, A fractional model for the dynamics of TB virus, *Chaos Solitons Fractals*, **116** (2018), 63–71.
[34] S. Ullah, M. Altaf Khan and M. Farooq, A new fractional model for the dynamics of the hepatitis B virus using the Caputo-Fabrizio derivative, *The European Physical Journal Plus*, **133** (2018), 237.
[35] S. Ullah, M. Altaf Khan, M. Farooq, Z. Hammouch and D. Baleanu, A fractional model for the dynamics of tuberculosis infection using Caputo-Fabrizio derivative, *Discrete & Continuous Dynamical Systems-S*, **13** (2020), 975–993.

Received December 2019; revised January 2020.

E-mail address: yonesesmaeelzade@gmail.com
E-mail address: Hsafdari@sru.ac.ir
E-mail address: yaqub.azari@gmail.com, yaqub.azari@sru.ac.ir
E-mail address: jafari.usern@gmail.com
E-mail address: dumitru@cankaya.edu.tr

View publication stats